Di-*tert*-butyl Phosphate Complexes of Titanium

Claus G. Lugmair and T. Don Tilley*

Department of Chemistry, University of California at Berkeley, Berkeley, California 94720-1460, and Chemical Sciences Division, Lawrence Berkeley Laboratory, 1 Cyclotron Road, Berkeley, California 94720

Received October 23, 1997

Reactions of 1 equiv of $HO(O)P(O^tBu)_2$ with $Ti(OR)_4$ (R = Et, ^{i}Pr) give the new molecular titanium phosphates $[Ti(OR)_3O_2P(O^tBu)_2]_n$ (**1**, R = Et; **2**, R = ^{i}Pr). In the solid state, **2** exists as a centrosymmetric dimer containing five-coordinate metal centers. Addition of 2 equiv of KOEt to an ethanol solution of **1** led to the formation of $[Ti_2K(OEt)_8O_2P(O^tBu)_2]_2$ (**3**) and 1 equiv of $KO_2P(O^tBu)_2$. A single-crystal X-ray structure analysis of **3** revealed that this complex exists in the solid state as a centrosymmetric dimer containing two Ti-centered, face-sharing pseudooctahedra in the unique half of the dimer. Addition of 2 equiv of KO^{i}Pr to a 2-propanol solution of **2** led to the formation of $KO_2P(O^tBu)_2$ (**4**) and $Ti(O^iPr)_4$ in high yield. Cooling a 2-propanol solution of **4** to −80 °C led to crystallization of the solvated tetramer $[\mathbf{4}\cdot HO^iPr_3]_4$ (mp = −30 °C). A single-crystal X-ray structure analysis revealed that this tetramer possesses a cubelike K_4O_4 core with 4-fold improper rotation symmetry. Multinuclear NMR studies of **1**−**3** show that the structures of these complexes are dynamic in solution. Crystals of **4** are tetragonal ($P4_2/n$) with a = 18.6261(3) Å, c = 14.7114(3) Å, and Z = 8.

Introduction

Alkali-metal-containing titanium phosphate materials have been studied for a variety of applications. Lamellar titanium phosphates have been shown to have ion exchange properties for numerous alkali- and alkaline-earth-metal ions.[1] Nasicon-type phosphates ($KTi_2(PO_4)_3$) have been shown to be fast ion conductors[2] and low thermal expansion ceramics.[3] Potassium titanyl phosphate ($KTiOPO_4$ or KTP) has been studied extensively as a nonlinear optical material[4,5] as well as a structural archetype from which numerous related structures have been derived.[5]

In contrast, the chemistry of molecular titanium phosphates, which might serve as precursors to solid-state materials, is quite limited. Early work in this area afforded insoluble titanium dialky phosphates, which were proposed to be polymers and/or three-dimensional networks.[6] Starting from titanium halides, amides, and siloxides, Thorn and Harlow have recently prepared and structurally characterized the first well-defined molecular titanium phosphate complexes.[7] Also, several reports have appeared describing the preparation of KTP films from dissolved mixtures of Ti alkoxides, phosphate esters, and K alkoxides.[8,9] The existence of a molecular alkoxide complex containing potassium, titanium, and phosphorus in a 1:1:1 stoichiometry was inferred from NMR spectroscopy and a solution molecular weight determination; however, the oily nature of this material prevented its full characterization.[9]

We have been interested in the preparation and study of "single source" molecular precursors of the type $M[OSi(O^tBu)_3]_n$, which are transformed under mild thermolysis to carbon-free, homogeneous silicate materials.[10] We have recently extended this approach to the preparation of phosphate materials by employing the di-*tert*-butyl phosphate ligand, $^-O_2P(O^tBu)_2$.[11] Use of this ligand led to the isolation of several zinc phosphates which could be transformed at low temperatures to zinc phosphate materials. In this contribution we describe the synthesis of two new members of a small class of compounds involving phosphate coordination to titanium, $[Ti(OR)_3O_2P(O^tBu)_2]_n$ (**1**, R = Et; **2**, R = ^{i}Pr). The reaction of KOEt with **1** resulted in formation of the crystalline potassium titanium

(1) (a) *Inorganic Ion Exchange Materials*; Clearfield, A., Eds.; CRC Press: Boca Raton, FL, 1982. (b) Alvarez, C.; Llavona, R.; Garcia, J. R.; Suarez, M.; Rodriguez, J. *Inorg. Chem.* **1987**, *26*, 1045.
(2) (a) Wang, S.; Hwu, S. J. *J. Solid State Chem.* **1991**, *90*, 377. (b) Wang, B.; Greenblatt, M.; Wang, S.; Hwu, S. J. *Chem. Mater.* **1993**, *5*, 32.
(3) Limaye, S. Y.; Agrawal, D. K.; McKinstry, H. A. *J. Am. Ceram. Soc.* **1987**, *70*, C232.
(4) (a) Munowitz, M.; Jarman, R. H.; Harrison, J. F. *Chem. Mater.* **1992**, *4*, 1296. (b) Hagerman, M. E.; Poeppelmeier, K. R. *Chem. Mater.* **1995**, *7*, 602.
(5) (a) Stucky, G. D.; Phillips, M. L. F.; Gier, T. E. *Chem. Mater.* **1989**, *1*, 492. (b) Harrison, W. T. A.; Phillips, M. L. F.; Stucky, G. D. *Chem. Mater.* **1995**, *7*, 1849. (c) Harrison, W. T. A.; Phillips, M. L. F.; Stucky, G. D. *Chem. Mater.* **1997**, *9*, 1138.
(6) (a) Dahl, G. H.; Block, B. P. *Inorg. Chem.* **1967**, *6*, 1439. (b) Mikulski, C. M.; Karayannis, N. M.; Strocko, M. J.; Pytlewski, L. L.; Labes, M. M. *Inorg. Chem.* **1970**, *9*, 2053. (c) Mikulski, C. M.; Tran, T.; Pytlewski, L. L.; Karayannis, N. M. *J. Inorg. Nucl. Chem.* **1979**, *41*, 1671.
(7) Thorn, D. L.; Harlow, R. L. *Inorg. Chem.* **1992**, *31*, 3917.
(8) (a) Harmer, M. A.; Roelofs, M. G. In *Better Ceramics Through Chemistry;* Materials Research Society Symposia Proceedings Vol. 271; Hampden-Smith, M. J., Klemperer, W. G., Brinker, C. J., Eds.; Materials Research Society: Pittsburgh, PA, 1992; p 389. (b) Schmutz, C.; Basset, E.; Barboux, P.; Maquet, J. *J. Mater. Chem.* **1993**, *3*, 393.
(9) (a) Hirano, S. I.; Yogo, T.; Kikuta, K. I.; Noda, K. I.; Ichida, M.; Nakamura, A. *J. Am. Ceram. Soc.* **1995**, *78*, 2956. (b) Noda, K. I.; Sakamoto, W.; Kikuta, K. I.; Yogo, T.; Hirano, S. I. *Chem. Mater.* **1997**, *9*, 2174.
(10) (a) Terry, K. W.; Tilley, T. D. *Chem. Mater.* **1991**, *3*, 1001. (b) Terry, K. W.; Gantzel, P. K.; Tilley, T. D. *Chem. Mater.* **1992**, *4*, 1290. (c) Terry, K. W.; Gantzel, P. K.; Tilley, T. D. *Inorg. Chem.* **1993**, *32*, 5402. (d) Terry, K. W.; Lugmair, C. G.; Gantzel, P. K.; Tilley, T. D. *Chem. Mater.* **1996**, *8*, 274. (e) Su, K.; Tilley, T. D. *Chem. Mater.* **1997**, *9*, 588. (f) Su, K.; Tilley, T. D.; Sailor, M. J. *J. Am. Chem. Soc.* **1996**, *118*, 3459. (g) Terry, K. W.; Lugmair, C. G.; Tilley, T. D. *J. Am. Chem. Soc.* **1997**, *119*, 9745.
(11) Lugmair, C. G.; Tilley, T. D.; Rheingold, A. L. *Chem. Mater.* **1997**, *9*, 339.

S0020-1669(97)01347-5 CCC: $15.00
Published on Web 03/17/1998

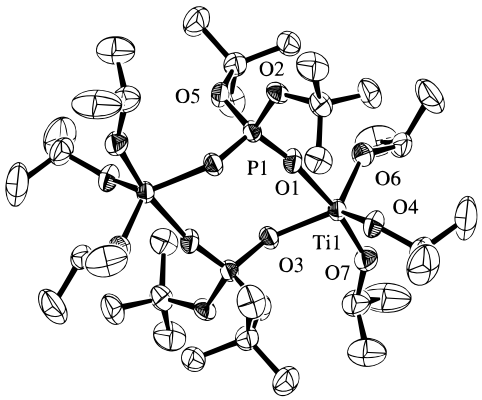

Figure 1. ORTEP view of **2**. Hydrogen atoms have been removed for clarity. Thermal ellipsoids are drawn at 50% probability.

phosphate complex $[Ti_2K(OEt)_8O_2P(O^tBu)_2]_2$ (**3**). However, the analogous reaction between KO^iPr and **2** resulted in conversion to $Ti(O^iPr)_4$ and $KO_2P(O^tBu)_2$.

Results

Reaction of 1 equiv of $HO(O)P(O^tBu)_2$[12] with $Ti(OR)_4$ (R = Et, ^{i}Pr) in pentane afforded the new titanium phosphates $[Ti(OR)_3O_2P(O^tBu)_2]_n$ (**1**: R = Et; **2**: R = ^{i}Pr) in good yields as colorless crystalline compounds (eq 1). The analogous reaction

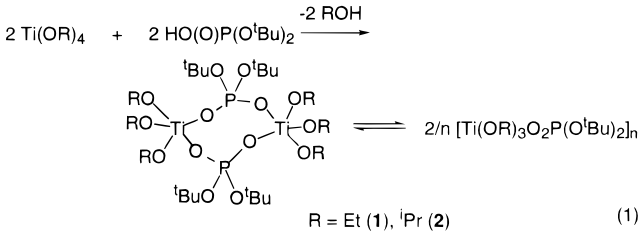

(1)

with $Ti(O^tBu)_4$ did not produce an isolable compound. On the basis of NMR data (vide infra), it appears that both **1** and **2** exist in solution as equilibrium mixtures of species with varying degrees of association. On the basis of the solid-state structure of **2**, we assume that dimeric structures are adopted to some degree by both compounds in solution.

Compound **2** forms large, colorless diamond-shaped crystals from pentane at −80 °C. These crystals become opaque within minutes when warmed to room temperature, and bulk samples display no diffraction peaks in their room temperature XRD spectra. This phenomenon is probably due to a phase change rather than desolvation (the crystals do not contain solvent) or decomposition (the compound is stable at room temperature). Compound **2** was found to be a centrosymmetric dimer in the solid state by single-crystal X-ray structure analysis (Figure 1). The titanium atoms are five coordinate with trigonal bipyramidal geometries. The O(1)−Ti(1)−O(7) angle is 170.1(1)°, and the sum of O−Ti−O angles involving the equatorial oxygens (O(3), O(4), and O(6)) is 358.8°. The Ti−O−P angle involving the oxygen atom in an axial position is 169.4(1)°, whereas the Ti−O−P angle involving the equatorial oxygen atom is only 132.3(1)°. The Ti−OP bond lengths are very similar [Ti(1)−O(1) = 2.048(2) Å; Ti(1)−O(3) = 1.997(2) Å].

In benzene-d_6 the ^{1}H NMR spectrum of **2** contains two sets of broad resonances for the O^{i}Pr groups in a 3:1 ratio and two barely resolved resonances for the O^{t}Bu groups. The ^{13}C and ^{31}P NMR spectra also reflect the presence of two $O_2P(O^tBu)_2$ environments. The ^{1}H NMR spectrum of **2** in toluene-d_8 contains three sets of O^{i}Pr resonances (in a 1:8:1 ratio) and three O^{t}Bu resonances over the temperature range of −50 to −20 °C. The appearance of these spectra are constant over this temperature range. Above 30 °C, only one resonance corresponding to the O^{t}Bu groups is observed, and resonances for the different O^{i}Pr environments become broad and are no longer resolved. The solution behavior of **2** indicates that the structure of this complex is dynamic in solution (the observed changes with temperature are reversible), and above 30 °C interconversion between various species (e.g., monomer, dimer, etc.) is rapid on the NMR time scale.

Complex **1** forms large cube-shaped crystals from pentane at −30 °C which analyze according to the empirical formula $Ti(OEt)_3O_2P(O^tBu)_2$. The room-temperature ^{1}H NMR spectrum of **1** reveals two sets of sharp resonances for the OEt groups, in a 1:2 ratio, and a single resonance for the O^{t}Bu groups. However, the ^{13}C NMR spectrum reveals two sets of resonances for both the OEt and O^{t}Bu groups. The ^{31}P NMR spectrum contains two major resonances and four smaller peaks. This indicates that **1** also adopts several structural forms in solution at room temperature. No significant change in the appearance of the ^{1}H NMR spectrum occurs upon cooling the sample to −80 °C. Above 70 °C, only one set of resonances corresponding to the −OEt groups is observed, signifying rapid interconversions of isomers and/or species with different degrees of association. Solution molecular weight determinations of **1** (by vapor diffusion) gave inconsistent results. It seems unlikely that some of the resonances in the NMR spectra are due to impurities, since the spectra did not change during eight recrystallizations of **1** using pentane and dichloromethane as solvents.

An attempt was made to prepare an alkoxide KTP precursor containing titanium, phosphorus, and potassium in a 1:1:1 stoichiometry. Combination of ethanol solutions of 2 equiv of KOEt and **1** led to a clear solution. Removal of the solvent and extraction of the remaining solid with pentane led to isolation of a complex which was formulated on the basis of combustion analyses and X-ray crystallography as $[Ti_2K(OEt)_8O_2P(O^tBu)_2]_2$ (**3**). The remaining insoluble material was found to be $KO_2P(O^tBu)_2$ (by IR spectroscopy; eq 2).

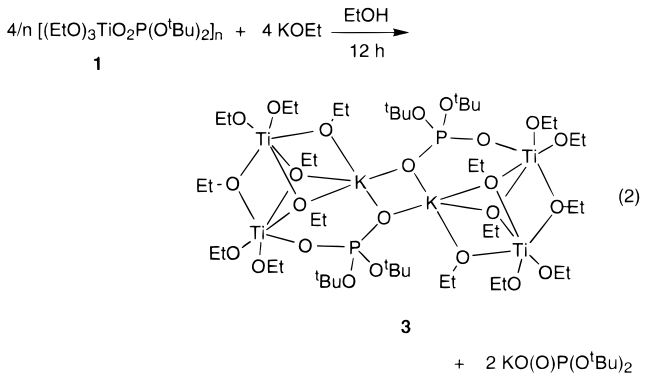

(2)

A single-crystal X-ray structure analysis of **3** revealed that this complex is a centrosymmetric dimer in the solid state (Figure 2). The two Ti atoms in the unique half of the dimer are bridged by three ethoxy groups, two of which also bridge to a potassium atom. The 6-fold coordination of Ti(1) is completed by two terminal OEt ligands and one oxygen atom of the $O_2P(O^tBu)_2$ group. The other oxygen atom of the phosphate ligand bridges the K atoms in each half of the dimer. Two terminal ethoxide ligands and a Ti(μ-OEt)K linkage complete the coordination sphere of Ti(2). The fragment containing

(12) Goldwhite, H.; Saunders: B. C. *J. Chem. Soc.* **1957**, 2409.

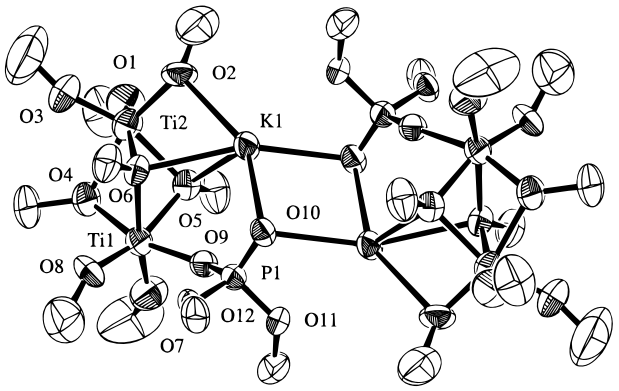

Figure 2. ORTEP view of **3.** Methyl groups have been removed for clarity. Thermal ellipsoids are drawn at 50% probability.

the two Ti atoms can be viewed as face-sharing octahedra, although the O−Ti−O angles deviate by as much as 21.6° from the ideal values. The Ti(1)···Ti(2) distance in this fragment (2.969(3) Å) is similar to the Ti···Ti distances of 3.028(2) Å in $[Ti_2(OEt)_8Cl]_2Mg_2(\mu\text{-}Cl)_2$[13a] and 3.100 Å in $[Ti_2(OEt)_9]YCl_2$,[13b] which also contain face-sharing pseudooctahedra. In compound **3**, all the Ti−O bond distances involving Ti(1) are slightly shorter than the bond distances to Ti(2). As expected, the Ti−OEt bond distances increase as the coordination number of the oxygen atom increases: Ti−O < Ti−(μ_2-O) < Ti−(μ_3-O). The K atom is coordinated by five oxygen atoms at normal K−O bond distances [2.694(6)−2.787(6) Å].[14] The coordination sphere of K(1) also includes O(9) and O(11)*, which exhibit significantly longer contacts to potassium [K(1)−O(9) = 3.099(6) Å; K(1)−O(11)* = 2.999(6) Å]. A powder XRD pattern obtained from a bulk sample of **3** matched the powder pattern calculated from the single-crystal data, indicating the presence of only one crystalline phase in this sample.

The solid-state structure of compound **3** contains five unique OEt environments. However, the room temperature ^{1}H NMR spectrum of **3** contains only a broad peak with a shoulder corresponding to the methylene protons of the OEt groups. The room-temperature ^{13}C NMR spectrum reveals two pairs of broad resonances resulting from the OEt groups. Above 40 °C, the ^{1}H NMR spectrum exhibits one pair of sharp resonances for the OEt groups signifying rapid exchange between the various sites. Between −40 and −50 °C, four overlapping triplets are observed for the methyl groups of the OEt ligands, indicating that dynamic processes for **3** have been substantially slowed.

An attempt was also made to prepare a potassium-containing complex from **2**. However, the reaction of 2 equiv of KO^{i}Pr with **2** in ^{i}PrOH led to isolation of $KO_2P(O^tBu)_2$ and $Ti(O^iPr)_4$ in good yields (eq 3). If the reaction mixture is concentrated

$$[(^iPrO)_3TiO_2P(O^tBu)_2]_2 \;(\mathbf{2}) + 2\,KO^iPr \xrightarrow[12\ h]{^iPrOH} 2\,Ti(O^iPr)_4 + 2\,KO(O)P(O^tBu)_2\;(\mathbf{4}) \qquad (3)$$

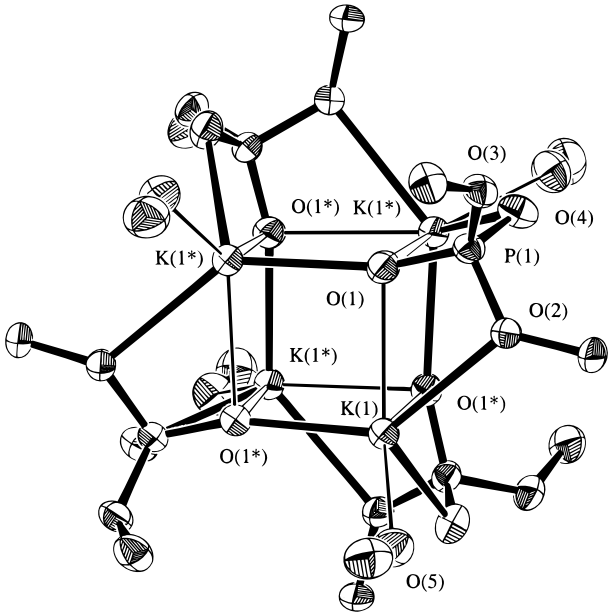

Figure 3. ORTEP view of the tetramer of **4**·3HO^{i}Pr. Two molecules of HO^{i}Pr per monomer, which interact with the cube only via hydrogen bonds, have been removed. The methyl groups have also been removed for clarity. Thermal ellipsoids are drawn at 50% probability.

and cooled to −80 °C, crystals of $KO_2P(O^tBu)_2$ form over several weeks. The synthesis of this compound has been previously reported.[15]

A single-crystal X-ray structure analysis reveals that $KO_2P(O^tBu)_2$ (**4**) exists in the solid state as a tetramer with a cubelike core (Figure 3). The structure contains 3 equiv of HO^{i}Pr per phosphate, leading to a low melting point for the crystals (−30 °C). Alternating cube corners are occupied by K atoms which are all related by a 4-fold improper rotation axis running through the center of the cube and parallel to the four hollow bonds shown in the ORTEP diagram (Figure 3). Oxygen atoms of the $O_2P(O^tBu)_2$ group, O(1), occupy the other four corners of the cube. A second oxygen atom of each $O_2P(O^tBu)_2$ group coordinates to potassium, forming a bridge across the cube edge. One of the O^{t}Bu groups also coordinates to a K atom, forming a second type of bridge across cube edges. The coordination number for K is brought to 6 by a terminally bound HO^{i}Pr molecule. The two molecules of HO^{i}Pr not shown in Figure 3 are involved in hydrogen-bonding interactions with each other and with O(5) and O(4)* [O(5)···O(6) = 2.768(4) Å; O(6)···O(7) = 2.666(4) Å; O(7)···O(4)* = 2.657(4) Å]. These two HO^{i}Pr molecules do not interact with the K atoms [K(1)···O(6) = 4.602(3) Å; K(1)···O(7) = 4.266(4) Å]. There are three unique K−O distances along the cube edges, 2.642(3), 2.789(3), and 3.201(2) Å, which are drawn as thick, thin, and hollow bonds, respectively (Figure 3). The shortest K−O distance (2.642(3) Å) is along the cube edge that is unsupported by any bridging interaction. The cube edge of intermediate length (2.789(3) Å) is bridged by P and an alkoxy O atom. The cube edge with the longest K−O distance is bridged by both P and O atoms. The bond angles associated with the cube core are close to 90°, the K−O−K angles [92.21(8)−98.67(7)°] being slightly larger than the O−K−O angles [81.66(7)−86.55(8)°].

Discussion

The metal−organic complexes $[Ti(OR)_3O_2P(O^tBu)_2]_n$ (**1**, R = Et; **2**, R = ^{i}Pr) represent rare examples of molecular titanium

(13) (a) Malpezzi, L.; Zucchini, U.; Dall'Occo, T. *Inorg. Chim. Acta* **1991**, *180*, 245. (b) Veith, M.; Mathur, S.; Huch, V. *Inorg. Chem.* **1997**, *36*, 2391.

(14) (a) Chisholm, M. H.; Drake, S. R.; Naiini, A. A.; Streib, W. E. *Polyhedron*, **1991**, *10*, 337. (b) Boyle, T. J.; Bradley, D. C.; Hampden-Smith, M. J.; Patel, A.; Ziller, J. W. *Inorg. Chem.* **1995**, *34*, 5893. (c) Teff, D. J.; Huffman, J. C.; Caulton, K. G. *Inorg. Chem.* **1994**, *33*, 6289. (d) Meese-Marktscheffel, J. A.; Weimann, R.; Schumann, H.; Gilje, J. W. *Inorg. Chem.* **1993**, *32*, 5894.

(15) Zwierzak, A.; Kluba, M. *Tetrahedron* **1971**, *27*, 3163.

phosphates. These complexes are formed cleanly by an alcohol-elimination reaction involving a titanium tetraalkoxide and di-*tert*-butyl phosphate. In the solid state, **2** adopts a dimeric structure that contains two Ti centers in trigonal bipyramidal coordination. Spectroscopy reveals that the structure of **2** is dynamic in solution, possibly due (at least in part) to a monomer−dimer equilibrium. The room-temperature ^{31}P NMR spectrum of **1** suggests that it exists in several forms in solution, and variable-temperature ^{1}H NMR spectroscopy indicates that the various species in solution readily interconvert at high temperature. We postulate that compound **1** exists as several oligomeric species in solution. These species may adopt structures with titanium centers linked by phosphate and/or μ_2-OEt bridges. Similar results were described by Hirano et al. for the reaction of Ti(OEt)$_4$ with HO$_2$P(O^{n}Bu)$_2$, which also led to complexes with dynamic behavior in solution.[9] A related reaction between Ti(OSiMe$_3$)$_4$ and HO$_2$P(O^{t}Bu)$_2$ gave an oxotitanium phosphate complex in good yield.[7] The latter complex possesses a cubic Ti$_4$O$_4$ core with one terminal OSiMe$_3$ group for each Ti atom and four O$_2$P(O^{t}Bu)$_2$ groups which bridge the Ti centers across the cube's face diagonals. Careful addition of either 0.5 or 1 equiv of water to a THF solution of **2** did not lead to the formation of an isolable oxotitanium cluster. Addition of 0.5 equiv of water to a benzene-d_6 solution of **2** shows that HO^{i}Pr is formed, as well as several new O$_2$P(O^{t}Bu)$_2$-containing species.

Addition of the appropriate potassium alkoxide to **1** and **2** did not lead to the formation of an isolable complex containing Ti, P, and K in a 1:1:1 stoichiometry. Instead, the phosphate ligand on Ti is readily displaced by the more basic alkoxide group, resulting in elimination of KO$_2$P(O^{t}Bu)$_2$. For **2**, this process is complete and Ti(O^{i}Pr)$_4$ is recovered in good yield. The reaction between **1** and KOEt results in the elimination of only 1 equiv of KO$_2$P(O^{t}Bu)$_2$ and formation of [Ti$_2$K(OEt)$_8$O$_2$P(O^{t}Bu)$_2$]$_2$ (**3**). In this case, the sterically less demanding OEt groups allow Ti to achieve a higher coordination number via bridging alkoxide groups. This results in saturation of the Ti coordination sphere with retention of the phosphate ligand. Although this complex exhibits dynamic behavior in solution, it does not decompose by the elimination of KO$_2$P(O^{t}Bu)$_2$ at elevated temperatures. Compound **3** did not undergo decomposition after heating to 70 °C for 10 min (by ^{1}H NMR spectroscopy). The chemistry of the O$_2$P(O^{t}Bu)$_2$ ligand in this system may be contrasted with that of O$_2$P(O^{n}Bu)$_2$, which gives a complex with the formula KTi(OEt)$_4$O$_2$P(O^{n}Bu)$_2$ which does not eliminate KO$_2$P(O^{n}Bu)$_2$ despite its highly dynamic behavior in solution.[9] Therefore the stability of titanium phosphate complexes seems to be highly sensitive to small changes in the steric properties of the ligands. The structure of **3**, consisting of face-sharing pseudooctahedra, is similar to the structures of heterometallic alkoxides such as [Ti$_2$(μ_3-OEt)$_2$(μ-OEt)$_2$(OEt)$_4$(μ-Cl)]$_2$Mg$_2$(μ-Cl)$_2$[13] and [Zr$_2$(μ_3-O^{i}Pr)$_2$(μ-O^{i}Pr)$_3$(O^{i}Pr)$_4$]$_2$Ba$_2$(μ-O^{i}Pr)$_2$[16] (Figure 4).

A single-crystal structural analysis of KO$_2$P(O^{t}Bu)$_2$ showed that it forms a solvated tetramer when crystallized from ^{i}PrOH. The cubelike K$_4$O$_4$ core of this molecule is a common molecular arrangement which has also been seen in potassium alkoxide and siloxide structures.[14a,17] In the alkoxides and siloxides, the K−O distances in the K$_4$O$_4$ core range between 2.6 and 2.8 Å. Two of the three sets of bond distances in the K$_4$O$_4$ core of **4** have a similar value. The third K−O distance, associated with the cube edge supported by the P−O(4) bond, is quite long (3.201(2) Å). The length of this contact is not too surprising considering that phosphate groups rarely chelate to a single metal center.[18] The insolubility of KO$_2$P(O^{t}Bu)$_2$ in less polar solvents such as toluene and THF indicates that it may be polymeric when not solvated by an alcohol.

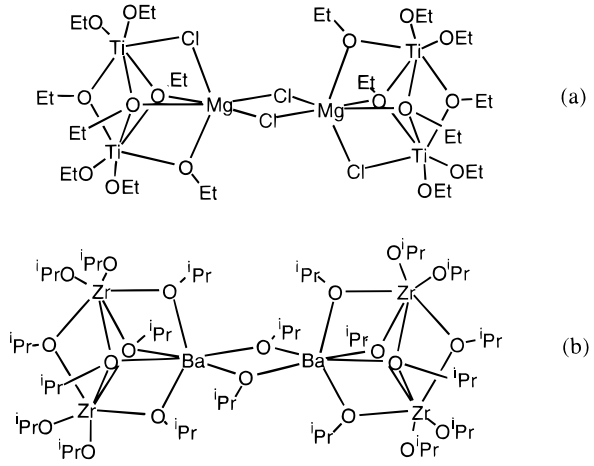

Figure 4. Molecular structure of (a) [Ti$_2$(μ_3-OEt)$_2$(μ-OEt)$_2$(OEt)$_4$(μ-Cl)]$_2$Mg$_2$(μ-Cl)$_2$ and (b) [Zr$_2$(μ_3-O^{i}Pr)$_2$(μ-O^{i}Pr)$_3$(O^{i}Pr)$_4$]$_2$ Ba$_2$(μ-O^{i}Pr)$_2$.

Experimental Section

General Methods. All manipulations were performed under a nitrogen atmosphere using standard Schlenk techniques or a Vacuum Atmospheres drybox. Diethyl ether, tetrahydrofuran, and pentane were distilled from sodium benzophenone under nitrogen. Toluene, benzene, and 2-propanol were distilled from sodium under nitrogen and then degassed. NMR spectra were recorded on a Bruker AMX-400 spectrometer at 400 (^{1}H), 100 (^{13}C), or 161 (^{31}P) MHz. Benzene-d_6 was used as the solvent for NMR studies unless specified otherwise. Infrared spectra were collected as Nujol mulls using CsI cells or as pressed pellets using KBr on a Mattson galaxy 3000 spectrometer. Powder X-ray diffraction was performed on a Siemens D5000 spectrometer. The compounds H(O)P(O^{t}Bu)$_2$[12] and KO(O)P(O^{t}Bu)$_2$[15] were prepared according to literature procedures.

[(EtO)$_3$TiO$_2$P(O^{t}Bu)$_2$]$_n$ (1). A pentane solution (30 mL) of HO(O)P(O^{t}Bu)$_2$ (0.92 g, 4.38 mmol) was added slowly to a pentane solution (30 mL) of Ti(OEt)$_4$ (1.00 g, 4.38 mmol) that had been cooled to −40 °C with a dry ice/ethanol bath. After the addition, the cold bath was removed and the reaction mixture stirred for 12 h. The solvent was removed under vacuum, and the resulting solid was extracted into pentane (25 mL). Concentration and cooling (−40 °C) of this solution afforded 1.42 g of **1** as colorless crystals in 83% yield. Anal. Calcd for C$_{14}$H$_{33}$O$_7$PTi: C, 42.87; H, 8.48. Found: C, 43.03; H, 8.60. IR (Nujol, CsI, cm^{-1}): 1469 m, 1447 w sh, 1393 m, 1369 s, 1323 w, 1252 m, 1243 m, 1175 m, 1159 m, 1121 s, 1047 s, 1003 s, 917 m, 895 m, 854 w, 834 m, 813 w, 616 s, 596 m sh, 560 m, 526 m sh, 483 s, 435 m, 412 w. ^{1}H NMR (400 MHz): δ 4.74 (q, 2 H, J = 7.1 Hz, OC*H*$_2$CH$_3$), 4.64 (q, 4 H, J = 6.7 Hz, OC*H*$_2$CH$_3$), 1.72 (t, 3 H, J = 7.1 Hz, OCH$_2$C*H*$_3$), 1.51 (s, 18 H, OC(CH$_3$)$_3$) 1.33 (t, 6 H, J = 6.9 Hz, OCH$_2$C*H*$_3$). ^{13}C{^{1}H} NMR (100 MHz): δ 80.05 (d, $^{2}J_{CP}$ = 5.0 Hz, O*C*(CH$_3$)$_3$), 77.89 (s, O*C*(CH$_3$)$_3$), 71.74 (s, O*C*H$_2$CH$_3$), 68.19 (s, O*C*H$_2$CH$_3$), 30.49 (d, $^{3}J_{CP}$ = 2.3 Hz, OC(*C*H$_3$)$_3$), 26.23 (s, OC(*C*H$_3$)$_3$), 19.50 (s, OCH$_2$*C*H$_3$), 19.08 (s, OCH$_2$*C*H$_3$). ^{31}P NMR (161.9 MHz): δ −8.29 (s), −8.40 (s), −8.48 (s), −8.88 (s), −10.04 (s), −13.56 (s).

[(^{i}PrO)$_3$TiO$_2$P(O^{t}Bu)$_2$]$_2$ (2). This compound was synthesized in 79% yield by the method described for **1**. Anal. Calcd for C$_{17}$H$_{39}$O$_7$PTi: C, 47.01; H, 9.05; P, 7.13. Found: C, 47.13; H, 9.06; P, 7.56. IR (KBr pellet, cm^{-1}): 2975 m, 2931 m, 2866 m, 1475 w sh, 1464 w, 1394 w, 1371 m, 1329 w, 1252 m, 1228 m, 1161 m sh, 1124 s, 1068 s, 1051 m sh, 1005 s, 850 m, 833 w sh, 709 w, 638 w, 625 w, 598 m,

(16) Caulton, K. G.; Hubert-Pfalzgraf, L. G. *Chem. Rev.* **1990**, *90*, 969.
(17) McGeary, M. J.; Folting, K.; Streib, W. E.; Huffman, J. C.; Caulton, K. G. *Polyhedron*, **1991**, *10*, 2699.
(18) Karayannis, N. M.; Mikulski, C. M.; Pytlewski, L. L. *Inorg. Chim. Acta Rev.* **1971**, 69.

Table 1. Selected Interatomic Distances (Å) and Angles (deg) for $[(^{i}PrO)_3TiO_2P(O^{t}Bu)_2]_2$ (**2**)

(a) Bond Distances

Ti(1)−O(1)	2.048(2)	Ti(1)−O(3)	1.997(2)
Ti(1)−O(4)	1.812(2)	Ti(1)−O(6)	1.796(2)
Ti(1)−O(7)	1.788(2)	P(1)−O(1)	1.490(2)
P(1)−O(2)	1.574(2)	P(1)−O(3)	1.513(2)
P(1)−O(5)	1.566(2)		

(b) Bond Angles

O(1)−Ti(1)−O(3)	82.40(8)	O(1)−Ti(1)−O(4)	88.37(9)
O(1)−Ti(1)−O(6)	89.10(10)	O(1)−Ti(1)−O(7)	170.1(1)
O(3)−Ti(1)−O(4)	128.79(10)	O(3)−Ti(1)−O(6)	118.7(1)
O(3)−Ti(1)−O(7)	87.90(10)	O(4)−Ti(1)−O(6)	111.3(1)
O(4)−Ti(1)−O(7)	96.3(1)	O(6)−Ti(1)−O(7)	97.2(1)
O(1)−P(1)−O(2)	110.5(1)	O(1)−P(1)−O(3)	115.6(1)
O(1)−P(1)−O(5)	113.8(1)	O(2)−P(1)−O(3)	108.8(1)
O(2)−P(1)−O(5)	103.2(1)	O(3)−P(1)−O(5)	104.1(1)
Ti(1)−O(1)−P(1)	169.4(1)	Ti(1)−O(3)−P(1)	132.3(1)

552 w, 499 w, 469 m. ^{1}H NMR (400 MHz): δ 5.20 (br s, OC*H*$(CH_3)_2$), 4.53 (br s, OC*H*$(CH_3)_2$), 1.60 (s, OC$(CH_3)_3$), 1.57 (s, OC$(CH_3)_3$), 1.38 (br s, OCH(C*H*$_3)_2$), 1.27 (br s, OCH(C*H*$_3)_2$). ^{13}C{^{1}H} NMR (100 MHz): δ 80.29 (s, O*C*$(CH_3)_3$), 79.86 (s, O*C*$(CH_3)_3$), 78.69 (s, O*C*H$(CH_3)_2$), 30.46 (s, OC(*C*H$_3)_3$), 30.27 (s, OC(*C*H$_3)_3$), 26.48 (s, OCH(*C*H$_3)_2$). ^{31}P NMR (161.9 MHz): δ −17.57 (s), −19.78 (s).

$[Ti_2K(OEt)_8O_2P(O^{t}Bu)_2]_2$ (3). An ethanol solution (15 mL) of **1** (0.71 g, 1.81 mmol) was added to an ethanol solution (15 mL) of KOEt (0.152 g, 1.81 mmol). The reaction mixture was stirred for 12 h. The solvent was then removed under reduced pressure, and the remaining white solid was kept under vacuum for 3 h. The solid was extracted with 25 mL of pentane leaving behind insoluble $KO_2P(O^{t}Bu)_2$ (IR spectroscopy). The pentane solution was concentrated and cooled to −40 °C to afford 0.45 g of **3** in 35% yield. Anal. Calcd for $C_{24}H_{58}KO_{12}PTi_2$: C, 40.91; H, 8.30; K, 4.39; P, 4.40. Found: C, 41.22; H, 8.44; K, 4.27; P, 5.08. IR (Nujol, CsI, cm^{-1}): 1447 m sh, 1392 m, 1369 m, 1352 w sh, 1255 m, 1242 w sh, 1220 m, 1153 m, 1109 m, 1098 m, 1066 s, 1003 s, 977 m, 918 m, 893 m, 831 m, 679 w, 600 s, 568 m sh, 492 w, 466 w, 442 w, 431 w. ^{1}H NMR (400 MHz): δ 4.63 (br, OC*H*$_2$CH$_3$), 1.50 (s, OC$(CH_3)_3$) 1.41 (br, OCH$_2$C*H*$_3$). ^{13}C-{^{1}H} NMR (100 MHz): δ 78.14 (br, O*C*$(CH_3)_3$), 69.90 (br, O*C*H$_2$-CH$_3$), 66.68 (br, OCH$_2$CH$_3$), 30.22 (d, $^3J_{CP}$ = 4.2 Hz, OC(*C*H$_3)_3$), 20.11 (br, OCH$_2$*C*H$_3$), 19.46 (br, OCH$_2$*C*H$_3$). ^{31}P NMR (161.9 MHz): δ −12.34 (s).

Reaction of 2 with KO^{i}Pr. Anhydrous 2-propanol (25 mL) was added to a flask containing KH (0.038 g, 0.95 mmol). After the KH had completely reacted with the solvent, a 2-propanol (15 mL) solution of **2** (0.414 g, 0.47 mmol) was added. After stirring of the reaction mixture for 12 h, the volatile material was removed under vacuum. Extraction of the remaining material with 20 mL of pentane yields $KO_2P(O^{t}Bu)_2$ as a white insoluble powder. Concentration of the filtrate under vacuum results in the isolation of Ti(O^{i}Pr)$_4$ in >90% yield (^{1}H NMR spectroscopy). If the crude reaction mixture is concentrated to ca. 10 mL and cooled to −80 °C, colorless crystals of **4** form within 3 days. After removal of the solvent by filtration, the crystals melt when warmed above −30 °C.

Crystallographic Structure Determinations. Crystallographic data are collected in Tables 1−4. Crystals of **2** were grown from a concentrated pentane solution at −80 °C. A colorless blocky crystal of dimensions 0.25 × 0.18 × 0.11 mm was mounted on a glass fiber using Paratone N hydrocarbon oil. Data were collected using a Siemens SMART diffractometer with a CCD area detector. A preliminary orientation matrix and unit cell parameters were determined by collecting 60 10-s frames, followed by spot integration and least-squares refinement. A hemisphere of data was collected using ω scans of 0.3° and a collection time of 30 s/frame. Frame data were integrated (*XY* spot spread = 1.60°; *Z* spot spread = 0.60°) using SAINT. The data were corrected for Lorentz and polarization effects. An absorption correction was performed using XPREP (μR = 0.20, T_{max} = 0.62, T_{min} = 0.58). The 9993 integrated reflections were averaged in point group 2/m to give 3864 unique reflections (R_{int} = 0.037). Of these 2679 reflections were considered observed ($I > 3.00\sigma(I)$). No decay correction was necessary. Inspection of the systematic absences uniquely defined the space group $P2_1/n$. The structure was solved using direct methods (SAPI91), expanded using Fourier techniques (DIRDIF92), and refined by full-matrix least-squares methods using teXsan software. The non-hydrogen atoms were refined anisotropically. The hydrogen atoms were included at calculated positions but not refined. The number of variable parameters was 235 giving a data/parameter ratio of 11.4. The maximum and minimum peaks on the final difference Fourier map corresponded to 0.23 and −0.31 e Å^{-3}: R = 0.038, R_w = 0.052, GOF = 1.66.

Table 2. Selected Interatomic Distances (Å) and Angles (deg) for $[Ti_2K(OEt)_8O_2P(O^{t}Bu)_2]_2$ (**3**)

(a) Bond Distances

Ti(1)−Ti(2)	2.969(3)	Ti(1)−K(1)	3.755(3)
Ti(1)−O(4)	1.992(7)	Ti(1)−O(5)	2.041(6)
Ti(1)−O(6)	2.072(6)	Ti(1)−O(7)	1.794(7)
Ti(1)−O(8)	1.773(7)	Ti(1)−O(9)	1.996(6)
Ti(2)−K(1)	3.522(3)	Ti(2)−O(1)	1.820(8)
Ti(2)−O(2)	1.872(7)	Ti(2)−O(3)	1.818(8)
Ti(2)−O(4)	2.143(7)	Ti(2)−O(5)	2.106(6)
Ti(2)−O(6)	2.075(6)	K(1)−K(1)	4.153(4)
K(1)−P(1)	3.430(3)	K(1)−P(1)	3.478(3)
K(1)−O(2)	2.743(7)	K(1)−O(5)	2.783(6)
K(1)−O(6)	2.787(6)	K(1)−O(9)	3.099(6)
K(1)−O(10)	2.768(6)	K(1)−O(10)	2.694(6)
K(1)−O(11)	2.999(6)	P(1)−O(9)	1.498(6)
P(1)−O(10)	1.468(6)	P(1)−O(11)	1.577(6)
P(1)−O(12)	1.571(6)		

(b) Bond Angles

O(4)−Ti(1)−O(5)	76.2(3)	O(4)−Ti(1)−O(6)	79.8(3)
O(4)−Ti(1)−O(7)	94.9(3)	O(4)−Ti(1)−O(8)	95.6(3)
O(4)−Ti(1)−O(9)	163.2(3)	O(5)−Ti(1)−O(6)	71.1(2)
O(5)−Ti(1)−O(7)	95.8(3)	O(5)−Ti(1)−O(8)	161.2(3)
O(5)−Ti(1)−O(9)	88.5(2)	O(6)−Ti(1)−O(7)	166.6(3)
O(6)−Ti(1)−O(8)	90.9(3)	O(6)−Ti(1)−O(9)	88.7(2)
O(7)−Ti(1)−O(8)	101.8(4)	O(7)−Ti(1)−O(9)	93.6(3)
O(8)−Ti(1)−O(9)	96.8(3)	O(1)−Ti(2)−O(2)	96.8(3)
O(1)−Ti(2)−O(3)	100.0(4)	O(1)−Ti(2)−O(4)	91.7(3)
O(1)−Ti(2)−O(5)	94.9(3)	O(1)−Ti(2)−O(6)	162.8(3)
O(2)−Ti(2)−O(3)	101.6(4)	O(2)−Ti(2)−O(4)	162.2(3)
O(2)−Ti(2)−O(5)	92.0(3)	O(2)−Ti(2)−O(6)	91.6(3)
O(3)−Ti(2)−O(4)	92.1(3)	O(3)−Ti(2)−O(5)	158.4(3)
O(3)−Ti(2)−O(6)	92.9(3)	O(4)−Ti(2)−O(5)	71.7(3)
O(4)−Ti(2)−O(6)	76.4(3)	O(5)−Ti(2)−O(6)	69.8(2)
O(2)−K(1)−O(5)	62.5(2)	O(2)−K(1)−O(6)	61.6(2)
O(2)−K(1)−O(9)	111.9(2)	O(2)−K(1)−O(10)	151.0(2)
O(2)−K(1)−O(10)	127.8(2)	O(2)−K(1)−O(11)	98.7(2)
O(5)−K(1)−O(6)	50.8(2)	O(5)−K(1)−O(9)	56.9(2)
O(5)−K(1)−O(10)	107.2(2)	O(5)−K(1)−O(10)	112.5(2)
O(5)−K(1)−O(11)	140.3(2)	O(6)−K(1)−O(9)	57.5(2)
O(6)−K(1)−O(10)	90.5(2)	O(6)−K(1)−O(10)	158.0(2)
O(6)−K(1)−O(11)	152.0(2)	O(9)−K(1)−O(10)	50.4(2)
O(9)−K(1)−O(10)	102.4(2)	O(9)−K(1)−O(11)	148.5(2)
O(10)−K(1)−O(10)	81.0(2)	O(10)−K(1)−O(11)	104.1(2)
O(10)−K(1)−O(11)	49.8(2)	O(9)−P(1)−O(11)	109.2(4)
O(9)−P(1)−O(10)	116.1(4)	O(10)−P(1)−O(11)	104.8(3)
O(9)−P(1)−O(12)	105.0(4)	O(11)−P(1)−O(12)	107.6(3)
O(10)−P(1)−O(12)	113.8(4)	Ti(1)−O(4)−Ti(2)	91.7(3)
Ti(2)−O(2)−K(1)	97.7(3)	Ti(1)−O(5)−K(1)	101.1(2)
Ti(1)−O(5)−Ti(2)	91.4(2)	Ti(1)−O(6)−Ti(2)	91.5(2)
Ti(2)−O(5)−K(1)	91.1(2)	Ti(2)−O(6)−K(1)	91.7(2)
Ti(1)−O(6)−K(1)	100.2(2)	Ti(1)−O(9)−K(1)	92.4(2)
K(1)−O(6)−C(9)	115.9(6)	K(1)−O(9)−P(1)	89.5(3)
Ti(1)−O(9)−P(1)	154.7(4)	K(1)−O(10)−P(1)	103.9(3)
K(1)−O(10)−K(1)	99.0(2)	K(1)−O(11)−P(1)	93.8(3)
K(1)−O(10)−P(1)	109.9(3)		

Crystals of **3** were grown from a concentrated pentane solution at −80 °C. A colorless needle crystal of dimensions 0.25 × 0.10 × 0.08 mm was mounted on a glass fiber using Paratone N hydrocarbon oil. Data were collected as described above. The data were corrected for Lorentz and polarization effects. An absorption correction was performed using XPREP (μR = 0.05, T_{max} = 0.88, T_{min} = 0.83). The 15 796 integrated reflections were averaged in point group 2/*m* to give

Table 3. Selected Interatomic Distances (Å) and Angles (deg) for $[KO_2P(O^tBu)_2(HO^iPr)_3]_4$ (**4**·3HO^{i}Pr)

(a) Bond Distances			
K(1)−K(1)	3.915(2)	K(1)−K(1)	4.447(1)
K(1)−K(1)	4.447(1)	K(1)−P(1)	3.443(1)
K(1)−P(1)	3.384(1)	K(1)−O(1)	2.789(3)
K(1)−O(1)	2.642(3)	K(1)−O(1)	3.201(2)
K(1)−O(2)	2.817(2)	K(1)−O(4)	2.664(2)
K(1)−O(5)	2.774(3)	P(1)−O(1)	1.491(3)
P(1)−O(2)	1.604(2)	P(1)−O(3)	1.588(2)
P(1)−O(4)	1.488(2)	O(2)−C(1)	1.472(4)
O(3)−C(5)	1.466(4)	O(5)−C(9)	1.424(5)
O(6)−C(12)	1.416(6)	O(7)−C(15)	1.327(5)
(b) Bond Angles			
O(1)−K(1)−O(1)	86.55(8)	O(1)−K(1)−O(1)	81.66(7)
O(1)−K(1)−O(2)	51.55(7)	O(1)−K(1)−O(4)	128.69(8)
O(1)−K(1)−O(5)	128.28(8)	O(1)−K(1)−O(1)	83.92(7)
O(1)−K(1)−O(2)	137.97(8)	O(1)−K(1)−O(4)	103.42(8)
O(1)−K(1)−O(5)	109.66(8)	O(1)−K(1)−O(2)	91.86(7)
O(1)−K(1)−O(4)	50.61(7)	O(1)−K(1)−O(5)	146.45(8)
O(2)−K(1)−O(4)	105.80(8)	O(2)−K(1)−O(5)	96.70(8)
O(4)−K(1)−O(5)	95.90(8)	O(1)−P(1)−O(2)	103.8(1)
O(1)−P(1)−O(3)	113.1(1)	O(1)−P(1)−O(4)	118.0(1)
O(2)−P(1)−O(3)	105.4(1)	O(2)−P(1)−O(4)	111.0(1)
O(3)−P(1)−O(4)	105.0(1)	K(1)−O(1)−K(1)	92.21(8)
K(1)−O(1)−K(1)	95.63(7)	K(1)−O(1)−P(1)	102.9(1)
K(1)−O(1)−K(1)	98.67(7)	K(1)−O(1)−P(1)	164.4(1)
K(1)−O(1)−P(1)	83.9(1)	K(1)−O(2)−P(1)	98.5(1)
K(1)−O(4)−P(1)	105.7(1)		

5554 unique reflections ($R_{int} = 0.059$). Of these 2774 reflections were considered observed ($I > 3.00\sigma(I)$). No decay correction was necessary. Inspection of the systematic absences uniquely defined the space group $P2_1/n$. The structure was solved using direct methods (SAPI91), expanded using Fourier techniques (DIRDIF92), and refined by full matrix least-squares methods using teXsan software. The non-hydrogen atoms were refined anisotropically. The hydrogen atoms were included at calculated positions but not refined. The number of variable parameters was 361 giving a data/parameter ratio of 7.68. The maximum and minimum peaks on the final difference Fourier map corresponded to 0.48 and −0.41 e Å^{-3}: $R = 0.066$, $R_w = 0.085$, GOF = 2.43.

Crystals of **4**·3HO^{i}Pr were grown from a concentrated 2-propanol solution at −80 °C. A colorless blocky crystal of dimensions 0.92 × 0.40 × 0.20 mm was mounted on a glass fiber using Paratone N hydrocarbon oil. Data were collected as described above with a collection time of 20 s/frame. Frame data was integrated (*XY* spot spread = 1.60°; *Z* spot spread = 0.60°) using SAINT. The data were corrected for Lorentz and polarization effects. An absorption correction was performed using XPREP ($\mu R = 0.1$, $T_{max} = 0.87$, $T_{min} = 0.62$).

Table 4. Crystallographic Data for Compounds **2**−**4**

	compound		
	2	**3**	**4**·3HO^{i}Pr
empirical formula	$C_{17}H_{39}O_7PTi$	$C_{24}H_{58}KO_{12}PTi_2$	$C_{17}H_{39}KO_7P$
fw	434.36	704.59	425.56
space group	$P2_1/n$	$P2_1/n$	$P4_1/n$
T, °C	−109	−89	−135
a, Å	13.1934(6)	9.5622(2)	18.6261(3)
b, Å	11.9751(5)	27.3300(4)	
c, Å	15.9864(7)	14.4630(3)	14.7114(3)
β, deg	102.917(1)	90.628(1)	
V, Å^3	2461.8(2)	3779.5(1)	5102.9(1)
Z	4	4	8
ρ(calc), g cm^{-3}	1.172	1.238	1.108
μ(Mo Kα), cm^{-1}	4.41	6.23	2.99
$R(F)$, %[a]	3.8	6.6	4.3
$R(wF)$, %[b]	5.2	8.5	5.5

[a] $R(F) = \sum||F_o| - |F_c||/|F_o|$. [b] $R(wF) = [\sum w(|F_o| - |F_c|)^2/\sum w(F_o)^2]^{1/2}$.

The 21 270 integrated reflections were averaged in point group 4/*m* to give 4068 unique reflections ($R_{int} = 0.081$). Of these 2395 reflections were considered observed ($I > 3.00\sigma(I)$). No decay correction was necessary. Inspection of the systematic absences uniquely defined the space group $P4_2/n$. The structure was solved using direct methods (SIR92) and refined by full-matrix least-squares methods using teXsan software. The non-hydrogen atoms were refined anisotropically. Hydrogen atoms were included for the −OH groups on the three 2-propanol molecules at locations where peaks were found in the Fourier difference map. These protons were not refined. The remaining hydrogen atoms were included at calculated positions but not refined. The number of variable parameters was 235 giving a data/parameter ratio of 10.19. The maximum and minimum peaks on the final difference Fourier map corresponded to 0.44 and −0.35 e Å^{-3}: $R = 0.043$, $R_w = 0.055$, GOF = 1.30.

Acknowledgment. This work was supported by the Director, Office of Energy Research, Office of Basic Energy Sciences, Chemical Sciences Division, of the U.S. Department of Energy under Contract No. DE-AC03-76SF00098. We also thank Dr. Fred Hollander of the departmental X-ray facility (CHEXRAY) for help in determining the crystal structures.

Supporting Information Available: Listings of crystal, data collection, and refinement parameters, atomic coordinates and *B* values, bond distances and angles, and anisotropic displacement parameters for **2**−**4** (16 pages). Ordering information is given on any current masthead page.

IC971347E